Activation of AMP-activated Protein Kinase Protects Against Homocysteine-Induced Apoptosis of Osteocytic MLO-Y4 Cells by Regulating the Expressions of NADPH oxidase 1 (Nox1) and Nox2

Ayumu Takeno, Ippei Kanazawa, Ken-ichiro Tanaka, Masakazu Notsu, Maki Yokomoto, Toru Yamaguchi, Toshitsugu Sugimoto

Internal Medicine 1,

Shimane University Faculty of Medicine,

89-1, Enya-cho, Izumo, Shimane 693-8501, Japan

E-mail address: Ayumu Takeno; atakeno@med.shimane-u.ac.jp

Ippei Kanazawa; ippei.k@med.shimane-u.ac.jp

Ken-ichiro Tanaka; ken1nai@med.shimane-u.ac.jp

Masakazu Notsu; mnotsu25@med.shimane-u.ac.jp

Maki Yokomoto; pinyan@med.shimane-u.ac.jp

Toru Yamaguchi; yamaguch@med.shimane-u.ac.jp

Toshitsugu Sugimoto; sugimoto@med.shimane-u.ac.jp

Correspondence and requests for reprints:

Ippei Kanazawa

Internal Medicine 1, Shimane University Faculty of Medicine

89-1, Enya-cho, Izumo, Shimane 693-8501, Japan

Phone: +81-853-20-2183, FAX: +81-853-23-8650

E-mail: ippei.k@med.shimane-u.ac.jp

Conflicts of Interest: None

Abstract

Background: Elevated plasma homocysteine (Hcy) level is associated with the risk of osteoporotic fracture. While Hcy increases oxidative stress, AMP-activated protein kinase (AMPK) activation ameliorates it. This study aimed to investigate whether Hcy induces apoptosis of osteocytic MLO-Y4 cells through regulating expressions of oxidant and anti-oxidant enzymes and determine the effects of AMPK activation by 5-aminoimidazole-4-carboxamide-1-β-D-ribofuranoside (AICAR) and metformin on the Hcy-induced apoptosis of the cells.

Results: DNA fragment ELISA and TUNEL staining assays showed that Hcy treatments (0.1–5.0 mM) induced apoptosis of MLO-Y4 cells in a dose-dependent manner. The detrimental effect of Hcy was partly but significantly reversed by an antioxidant (*N*-acetylcysteine) and NADPH oxidase (Nox) inhibitors (apocynin and diphenyleneiodonium). In addition, treatment with AICAR (0.05–0.1 mM) and metformin (10–100 µM) ameliorated Hcy-induced apoptosis of the cells. The favorable effect of metformin on Hcy-induced apoptosis was completely cancelled by an AMPK inhibitor Ara-A. Hcy increased the expression levels of Nox1 and Nox2, while it had no effects on the expressions of Nox4 or the anti-oxidant enzymes, superoxide dismutase 1 and 2. Hcy-induced increases in the expressions of Nox1 and Nox2 decreased significantly by treatments with AICAR.

Conclusion: These findings suggest that Hcy induces apoptosis of osteocytes by increasing the expressions of Nox1 and Nox2, and AMPK activation by AICAR and metformin effectively prevents the detrimental reactions. Thus, AMPK activation may be a potent therapeutic candidate for preventing Hcy-induced osteocyte apoptosis and the resulting bone fragility.

Keywords: homocysteine, osteocyte, AMP-activated protein kinase, oxidative stress, NADPH oxidase

Abbreviations

AMPK: AMP-activated protein kinase, AICAR: 5-aminoimidazole-4-carboxamide-1-β-D-ribofuranoside, Nox: NADPH oxidase, Hcy: homocysteine, SOD: superoxide dismutase, DPI: diphenyleneiodonium chloride, NAC: N-acetylcysteine, ROS: reactive oxygen species,

Introduction

Homocysteine (Hcy) is a sulfur-containing amino acid formed by the demethylation of methionine, and high plasma Hcy levels are often caused by vitamin B12 and folate insufficiency [1] and polymorphism in the gene encoding the folate-metabolising enzyme methylenetetrahydrofolate reductase [2, 3]. Accumulating evidence has shown that elevated plasma Hcy level is a risk factor for osteoporotic fracture [4-7]. In accordance with the epidemiological studies, previous animal studies have shown that diet-induced hyperhomocysteinemia decreases bone quality [8, 9]. However, the mechanisms underlying Hcy-induced bone fragility have not been completely elucidated thus far. Previous studies have shown that Hcy increases the apoptosis of osteoblast lineage cells such as bone marrow stromal cells [10] and osteoblasts [11]. Hcy is a potent pro-oxidant [12-14], it induces the apoptosis of bone marrow stromal cells by increasing oxidative stress [8]. Furthermore, Hcy suppresses the expression of lysyl oxidase in osteoblasts, resulting in inhibiting enzymatic collagen cross-links [15]. These findings indicate that Hcy has negative impacts on cell viability and function of osteoblasts.

AMP-activated protein kinase (AMPK) plays a pivotal role as an intracellular energy sensor and is associated with the regulation of appetite and glucose and fat metabolism [16]. Metformin is frequently used for the treatment of type 2 diabetes mellitus and is known to improve insulin sensitivity by activating AMPK. We previously showed that AMPK

5

activation by 5-aminoimidazole-4-carboxamide-1-β-D-ribofuranoside (AICAR), a pharmacological AMPK activator, and metformin stimulates the differentiation and mineralization of osteoblastic MC3T3-E1 cells [17]. In addition, *AMPK*-knockout mice show a significant reduction in bone volume [18]. Thus, AMPK may have positive effects on bone formation.

Oxidative stress is regulated by many oxidant and antioxidant enzymes. Oxidative stress is predominantly induced by NADPH oxidase (Nox) [19], one of the oxidant enzymes, and is prevented by antioxidant enzymes such as superoxide dismutase (SOD) [20]. Several studies have shown that AMPK activation ameliorates oxidative stress in various cells by regulating the activities of Nox and SOD [21-26]. However, whether AMPK activation decreases Hcy-induced oxidative stress by regulating oxidant-antioxidant enzymes in osteoblast lineage cells has not been clarified thus far.

Osteocytes are the most abundant cells in the bone, and they play important roles in coordinating the functions of osteoblasts and osteoclasts [27]. Estrogen deficiency [28] as well as mechanical loading [29] and glucocorticoid administration [30] are associated with apoptosis of osteocytes, resulting in increased bone fragility. However, to our best knowledge, no study has described the effects of Hcy and AMPK on osteocytes. Thus, the purpose of our study was to examine the effects of Hcy and AMPK activators on the apoptosis of osteocytic MLO-Y4 cells and on the expressions of Nox and SOD in the cells.

6

Materials and Methods

Reagents

Cell culture medium and supplements were purchased from GIBCO-BRL (Rockville, MD). AICAR was purchased from Cell Signaling (Beverly, MA). DL-homocysteine, *N*-acetyl-L-cysteine (NAC), and Ara-A were purchased from Sigma–Aldrich (St. Louis, MO). The Nox inhibitors apocynin and diphenyleneiodonium chloride (DPI) were purchased from Santa Cruz Biotech (Santa Cruz, CA) and Enzo Life Sciences (New York, NY), respectively. Metformin was kindly provided by Sumitomo Dainippon Pharma (Osaka, Japan). Antibodies against SOD1 and SOD2 were purchased from Abcam (Cambridge, UK). Rabbit monoclonal antibodies were from Sigma–Aldrich.

Cell cultures

MLO-Y4, a murine long bone-derived osteocytic cell line, was kindly provided by Dr. Lynda F. Bonewald. Cells were cultured on collagen-coated plates in α-minimum essential medium (α-MEM) supplemented with 10% fetal bovine serum (FBS) and 1% penicillin-streptomycin in 5% CO_2 at 37 °C. The medium was changed twice a week, and the cells were passaged when they were 80% confluent.

Apoptosis assay using a DNA fragment detection ELISA kit

Apoptosis was assessed by using Cell Death Detection ELISA^{plus} kit (Roche Applied Science, IN) according to the manufacturer's protocol. The cells were incubated in 96-well plates for 48 h, and Hcy, AICAR, metformin, and/or Ara-A were added at their specified concentrations after the cells were confluent. After incubation for 48 h, the cells were lysed using 200 μL of lysis buffer. After centrifugation, 20 μL of the supernatant was transferred to a streptavidin-coated microplate and exposed to anti-histone antibody (biotin-labeled) and anti-DNA antibody (peroxidase-conjugated) for 2 h at room temperature. Each well was washed 3 times with the incubation buffer, and antibody-nucleosome complexes bound to the microplate were determined spectrophotometrically using 2,2'-azino-bis(3-ethylbenzothiazoline-6-sulphonic acid) (ABTS). The absorbance measured using the kit was proportional to the degree of apoptosis. The results were expressed as relative to control.

TUNEL staining

We performed TUNEL staining using an in situ cell death detection kit (Roche, Germany) according to the manufacturer's protocol. Briefly, the cells were incubated in chamber slides. After the cells were confluent, we performed fixation, blocking, and permeabilization as indicated. The slides were immersed in TUNEL reaction mixture for 60 min at 37°C in a humidified atmosphere in the dark. The slides were analyzed using

optical microscopy. The average value of TUNEL-positive cells in one microscopic field (200×) was used to evaluate the degree of apoptosis. TUNEL-positive cells were counted in six randomly selected areas of TUNEL-stained slides, and the average value was calculated.

Reverse transcription PCR analysis to identify AMPK subunits

To investigate the mRNA expression of AMPK subunits (α1, α2, β1, β2, β3, γ1, γ2, and γ3) in MLO-Y4 cells, we performed reverse transcription (RT) PCR. Total RNA was extracted from the cultured MLO-Y4 cells using Trizol reagent (Invitrogen, San Diego, CA) according to the manufacturer's recommended protocol. We used 2 μg total RNA for the synthesis of single-stranded cDNA (cDNA synthesis kit; Invitrogen). We used the primers described in Table 1. The PCR conditions were as follows: denaturation at 95°C for 45 s; annealing at 60°C for α1 and α2, at 56°C for β1 and β2, and at 57°C for γ1, γ2, and γ3 for 30 s; and elongation at 72°C for 1 min for 35 cycles. The PCR products were separated by electrophoresis on a 1.8% agarose gel and were visualized using ethidium bromide staining with ultraviolet (UV) light using the Electronic UV trans-illuminator (Toyobo Co. Ltd., Tokyo, Japan).

Quantification of gene expression using real-time PCR

We used SYBR green chemistry to determine the mRNA levels of Nox1, Nox2,

Nox4, SOD1, and a housekeeping gene, *36B4*. The primer sequences used are described in Table 2. Real-time PCR was performed using 1 µL of cDNA in a 25 µL reaction volume with ABI PRISM 7000 (Applied Biosystems, Waltham, MA). The double-stranded DNA-specific dye SYBR Green I was incorporated into the PCR buffer provided in the SYBR Green Realtime PCR Master Mix (Toyobo Co. Ltd., Tokyo, Japan) to enable quantitative detection of the PCR product. The PCR conditions were 95°C for 15 min, 40 cycles of denaturation at 94°C for 15 s, and annealing and extension at 60°C for 1 min. *36B4* was used to normalize the differences in the efficiencies of reverse transcription.

Western blot analysis

For western blot analysis, the cells were plated in 6-well plates and cultured as described above. After the cells were confluent, they were treated with each agent for 48 h. The cells were rinsed with ice-cold PBS and scraped on ice into lysis buffer (BIO-RAD, Hercules, CA) containing 65.8 mM Tris-HCl (pH 6.8), 26.3% (w/v) glycerol, 2.1% SDS, and 0.01% bromophenol blue to which 2-mercaptoethanol was added to achieve a final concentration of 5%. The cell lysates were sonicated for 20 s. The cell lysates were electrophoresed using 10% SDS-PAGE and transferred to a nitrocellulose membrane (BIO-RAD, Hercules, CA). The blots were blocked with TBS containing 1% Tween 20 (BIO-RAD) and 3% bovine serum albumin (BSA) for 1 h at 4°C. Then, the blots were

10

incubated overnight at 4°C with gentle shaking with SOD1 or SOD2 antibodies at a dilution of 1:2000 and 1:5000, respectively. These blots were extensively washed with TBS containing 1% Tween 20 and were further incubated with a 1:2500 dilution of horseradish peroxidase-coupled rabbit antimouse IgG in TBS for 30 min at 4°C. The blots were then washed, and the signal was visualized using an enhanced chemiluminescence technique.

Statistics

Results are expressed as means ± standard error (SE). Statistical evaluations for differences between groups were performed using one-way ANOVA followed by Fisher's protected least significant difference. For all statistical tests, a value of $p < 0.05$ was considered a statistically significant difference.

Results

Hcy induced apoptosis of MLO-Y4 cells via increasing oxidative stress

The effects of Hcy on apoptosis of MLO-Y4 cells were examined using a DNA fragment detection ELISA kit. Incubation with Hcy at the indicated concentrations significantly increased the apoptosis in a dose-dependent manner (at least $p < 0.05$; Fig. 1A). Moreover, TUNEL staining confirmed that 5 mM Hcy significantly increased the apoptosis of MLO-Y4 cells (Fig. 1B and C).

An anti-oxidant (NAC) and Nox inhibitors, apocynin and DPI, ameliorated Hcy-induced apoptosis of MLO-Y4 cells

Further, to investigate whether oxidative stress is involved in Hcy-induced apoptosis, we examined the effect of NAC, an anti-oxidant, on Hcy-induced apoptosis. The apoptotic effect of Hcy was significantly decreased by co-incubation with 5 mM NAC ($p < 0.05$; Fig. 2A). These findings indicate that Hcy-induced apoptosis is mediated by oxidative stress.

Nox is an important enzyme involved in the induction of oxidative stress. To confirm the involvement of Nox in Hcy-induced apoptosis of MLO-Y4 cells, we examined whether the Nox inhibitors, apocynin and DPI, inhibit the Hcy-induced apoptosis of MLO-Y4 cells. Co-incubation of MLO-Y4 cells with 0.1 mM apocynin or 1.0 nM DPI and 5 mM Hcy partially but significantly inhibited Hcy-induced apoptosis of the cells ($p < 0.01$; Fig. 2B and

2C).

Expressions of AMPK subunits in MLO-Y4 cells

To date, no studies have shown that AMPK subunits are expressed in osteocytes. We examined the expressions of AMPK subunits by using RT-PCR. AMPK is a heteromeric protein that consists of three different subunits; an α catalytic subunit and β and γ regulatory subunits. In mammals, 7 genes encode AMPK subunits (*α1*, *α2*, *β1*, *β2*, *γ1*, *γ2*, and *γ3*) and can form 12 possible AMPK heteromers. RT-PCR showed that mRNAs of α1, α2, β1, β2, γ1, γ2, and γ3 were expressed in MLO-Y4 cells (Fig. 3A).

AMPK activators, AICAR and metformin, suppressed Hcy-induced apoptosis of MLO-Y4 cells

We investigated the effects of AICAR, a pharmacological activator of AMPK, on Hcy-induced apoptosis of the cells. DNA fragment detection ELISA showed that treatment with AICAR (0.05 and 0.1 mM) significantly decreased Hcy-induced apoptosis (at least $p<0.01$; Fig. 3B). In addition, TUNEL staining showed that treatment with 0.01 mM AICAR significantly inhibited Hcy-induced apoptosis ($p < 0.001$; Fig. 3C and 3D).

Further, we investigated the effects of AMPK activation by metformin on Hcy-induced apoptosis of MLO-Y4 cells. Metformin at a concentration of 10 and 100 μM

significantly decreased Hcy-induced apoptosis (at least p < 0.05; Fig. 3E). The favorable

effect of metformin on Hcy-induced apoptosis was significantly reversed by administration of

0.1 mM Ara-A, an AMPK inhibitor. These findings indicate that metformin decreases

Hcy-induced apoptosis via activation of AMPK.

AICAR prevented Hcy-induced Nox1 and Nox2 expressions

We investigated whether Hcy and AICAR affect the expressions of oxidant and

antioxidant enzymes. Real-time PCR showed that 5 mM Hcy significantly increased the

mRNA expression of Nox1 and Nox2 for 24 h (p < 0.01), and co-incubation with 0.1 mM

AICAR inhibited Hcy-induced upregulation of Nox1 and Nox2 mRNA (p < 0.01; Fig. 4A and

B). Incubation with Hcy did not affect the mRNA expression of Nox4 or SOD1 (Fig. 4C and

D). Western blot analysis showed that Hcy had no effect on the expressions of SOD1 and

SOD2 proteins (Fig. 4E).

14

Discussion

Several clinical studies have shown that moderate hyperhomocysteinemia increases the risk of osteoporotic fracture independent of the BMD [4-7], which suggests that the deterioration of bone quality may be a dominant cause of Hcy-induced bone fragility. Previous studies have shown that Hcy increases apoptosis of bone marrow stromal cells and osteoblasts [10, 11]; however, no studies have examined the effects of Hcy on osteocytes to date. Osteocytes play pivotal roles in regulating the functions of osteoblasts and osteoclasts [27], and apoptosis of osteocytes is closely associated with bone fragility [31, 32]. To our knowledge, this is the first study to report that Hcy induced the apoptosis of osteocytic MLO-Y4 cells. Therefore, the Hcy-induced apoptosis of osteocytes may be another possible cause of Hcy-induced bone fragility.

Oxidative stress is regulated by several enzymatic factors such as Nox, a dominant oxidative stress-inductive enzyme [19], and SOD, a major anti-oxidant enzyme [20]. Hcy increases oxidative stress in various cells [10, 12-14, 33]. For example, Sipkens *et al.* showed that Hcy induces apoptosis by increasing the activities of Nox2 and Nox4 in endothelial cells [34]. Further, the effect of oxidative stress on osteoblast function has been reported previously. Xu *et al.* showed that hydrogen peroxide increased the activity of Nox and reactive oxygen species (ROS), induced apoptosis, and suppressed the differentiation of osteoblastic MC3T3-E1 cells [35]. Moreover, Lee *et al.* showed that antimycin, a

15

mitochondrial electron transport inhibitor, increased ROS, decreased cell viability, and suppressed calcification in MC3T3-E1 cells, and these effects were inhibited by apocynin [36]. These findings indicate that Nox-mediated oxidative stress has a negative effect on osteoblasts. Apocynin is thought to interfere with the translocation of p47[phox], an organizer protein of the Nox2 complex, to the membrane [37]; therefore, Nox2 inhibition may be involved in the improvement of mitochondrial dysfunction-induced ROS. In the present study, we showed that Hcy increased the mRNA expression of Nox1 and Nox2, and Hcy-induced apoptosis was inhibited by Nox inhibitors. These findings indicate that Nox1 and Nox2 play important roles in Hcy-induced oxidative stress and apoptosis of osteocytes.

Previous studies showed that AMPK activation inhibits apoptosis by decreasing oxidative stress in several types of cells [21-23]. Chunfang *et al*. showed that Hcy increases oxidative stress and apoptosis by increasing the expression of Nox4 in endothelial progenitor cells, and AMPK activation decreases the effects of Hcy [38]. We showed for the first time that AMPK subunits are present in osteocytes and have anti-apoptotic effects. AMPK activation ameliorated the Hcy-induced expression of Nox1 and Nox2 and apoptosis of MLO-Y4 cells. NAC and Nox inhibitors partly inhibited the Hcy-induced apoptosis, while AICAR completely inhibited the Hcy-induced apoptosis. These findings suggest that other signaling pathways might be associated with the anti-apoptotic effects of AMPK. Previous studies have shown that PI3K/PKB and ERK signaling pathways and endoplasmic reticulum

stress are involved in the anti-apoptotic effects of AMPK activation in neutrophils [39] and endothelial cells [40]. Therefore, further studies are required to examine the roles of AMPK in osteocytes.

Accumulating evidence has shown that patients with type 2 diabetes mellitus have an increased BMD-independent risk of fractures [41, 42]. Although the mechanism underlying diabetes-related bone fragility is still unclear, high plasma Hcy levels are associated with the incidence of vertebral fractures and femoral neck fractures in patients with type 2 diabetes [43]. Thus, hyperhomocysteinemia may exacerbate bone fragility in patients with type 2 diabetes. Moreover, previous epidemiological studies have shown that treatment with biguanide is associated with a decreased risk of osteoporotic fracture [44, 45]. Our results and those from other studies showed that metformin increases the differentiation and mineralization of osteoblastic MC3T3-E1 cells [17, 46], and metformin increases bone volume in insulin-resistant mice [47] and ovariectomized rats [48]. In this study, we found that metformin inhibited Hcy-induced apoptosis of osteocytes via AMPK activation. Taken together, treatment with metformin may be beneficial for diabetes-related bone fragility by not only increasing bone formation but also improving bone fragility associated with osteocyte apoptosis.

In conclusion, our study showed for the first time that Hcy induced apoptosis of osteocytic MLO-Y4 cells via increasing the expressions of Nox1 and Nox2. Moreover,

AMPK activation ameliorated the detrimental effects of Hcy. Therefore, the apoptosis of osteocytes may be involved in the Hcy-induced bone fragility, and AMPK activators such as AICAR and metformin may be useful for preventing the risk of hyperhomocysteinemia-associated fracture. However, we used MLO-Y4 cell, a cell line of osteocyte, and relatively high concentration of Hcy compared to serum levels *in vivo*. To confirm the present findings, further *in vivo* experiments are needed in future.

References

[1]   Selhub J, Jacques PF, Wilson PW, Rush D, Rosenberg IH. Vitamin status and intake as primary determinants of homocysteinemia in an elderly population. JAMA 1993;270: 2693-8.

[2]   van Wijngaarden JP, Doets EL, Szczecinska A, Souverein OW, Duffy ME, Dullemeijer C, Cavelaars AE, Pietruszka B, Van't Veer P, Brzozowska A, Dhonukshe-Rutten RA, de Groot CP. Vitamin B12, folate, homocysteine, and bone health in adults and elderly people: a systematic review with meta-analyses. J Nutr Metab 2013;2013: 486186.

[3]   Wang H, Liu C. Association of MTHFR C667T polymorphism with bone mineral density and fracture risk: an updated meta-analysis. Osteoporos Int 2012;23: 2625-34.

[4]   van Meurs JB, Dhonukshe-Rutten RA, Pluijm SM, van der Klift M, de Jonge R, Lindemans J, de Groot LC, Hofman A, Witteman JC, van Leeuwen JP, Breteler MM, Lips P, Pols HA, Uitterlinden AG. Homocysteine levels and the risk of osteoporotic fracture. N Engl J Med 2004;350: 2033-41.

[5]   McLean RR, Jacques PF, Selhub J, Tucker KL, Samelson EJ, Broe KE, Hannan MT, Cupples LA, Kiel DP. Homocysteine as a predictive factor for hip fracture in older persons. N Engl J Med 2004;350: 2042-9.

[6]   Sato Y, Iwamoto J, Kanoko T, Satoh K. Homocysteine as a predictive factor for hip fracture in elderly women with Parkinson's disease. Am J Med 2005;118: 1250-5.

[7]   Yang J, Hu X, Zhang Q, Cao H, Wang J, Liu B. Homocysteine level and risk of fracture: A meta-analysis and systematic review. Bone 2012;51: 376-82.

[8]   Herrmann M, Wildemann B, Claes L, Klohs S, Ohnmacht M, Taban-Shomal O, Hubner U, Pexa A, Umanskaya N, Herrmann W. Experimental hyperhomocysteinemia reduces bone quality in rats. Clin Chem 2007;53: 1455-61.

[9]   Herrmann M, Tami A, Wildemann B, Wolny M, Wagner A, Schorr H, Taban-Shomal O, Umanskaya N, Ross S, Garcia P, Hubner U, Herrmann W. Hyperhomocysteinemia induces a tissue specific accumulation of homocysteine in bone by collagen binding and adversely affects bone. Bone 2009;44: 467-75.

[10]   Kim DJ, Koh JM, Lee O, Kim NJ, Lee YS, Kim YS, Park JY, Lee KU, Kim GS. Homocysteine enhances apoptosis in human bone marrow stromal cells. Bone 2006;39: 582-90.

[11]   Park SJ, Kim KJ, Kim WU, Oh IH, Cho CS. Involvement of endoplasmic reticulum stress in homocysteine-induced apoptosis of osteoblastic cells. J Bone Miner Metab 2012;30: 474-84.

[12]   Voutilainen S, Morrow JD, Roberts LJ, 2nd, Alfthan G, Alho H, Nyyssonen K, Salonen JT. Enhanced in vivo lipid peroxidation at elevated plasma total homocysteine levels. Arterioscler Thromb Vasc Biol 1999;19: 1263-6.

[13]   Eberhardt RT, Forgione MA, Cap A, Leopold JA, Rudd MA, Trolliet M, Heydrick S, Stark R, Klings ES, Moldovan NI, Yaghoubi M, Goldschmidt-Clermont PJ, Farber HW, Cohen R, Loscalzo J. Endothelial dysfunction in a murine model of mild hyperhomocyst(e)inemia. J Clin

Invest 2000;106: 483-91.

[14]   Lentz SR. Homocysteine and vascular dysfunction. Life Sci 1997;61: 1205-15.

[15]   Thaler R, Agsten M, Spitzer S, Paschalis EP, Karlic H, Klaushofer K, Varga F. Homocysteine suppresses the expression of the collagen cross-linker lysyl oxidase involving IL-6, Fli1, and epigenetic DNA methylation. J Biol Chem 2011;286: 5578-88.

[16]   Kola B, Boscaro M, Rutter GA, Grossman AB, Korbonits M. Expanding role of AMPK in endocrinology. Trends Endocrinol Metab 2006;17: 205-15.

[17]   Kanazawa I, Yamaguchi T, Yano S, Yamauchi M, Yamamoto M, Sugimoto T. Adiponectin and AMP kinase activator stimulate proliferation, differentiation, and mineralization of osteoblastic MC3T3-E1 cells. BMC Cell Biol 2007;8: 51.

[18]   Shah M, Kola B, Bataveljic A, Arnett TR, Viollet B, Saxon L, Korbonits M, Chenu C. AMP-activated protein kinase (AMPK) activation regulates in vitro bone formation and bone mass. Bone 2010;47: 309-19.

[19]   Brown DI, Griendling KK. Nox proteins in signal transduction. Free Radic Biol Med 2009;47: 1239-53.

[20]   Perry JJ, Shin DS, Getzoff ED, Tainer JA. The structural biochemistry of the superoxide dismutases. Biochim Biophys Acta 2010;1804: 245-62.

[21]   Qiu G, Wan R, Hu J, Mattson MP, Spangler E, Liu S, Yau SY, Lee TM, Gleichmann M, Ingram DK, So KF, Zou S. Adiponectin protects rat hippocampal neurons against excitotoxicity. Age (Dordr) 2011;33: 155-65.

[22]   Kim JE, Kim YW, Lee IK, Kim JY, Kang YJ, Park SY. AMP-activated protein kinase activation by 5-aminoimidazole-4-carboxamide-1-beta-D-ribofuranoside (AICAR) inhibits palmitate-induced endothelial cell apoptosis through reactive oxygen species suppression. J Pharmacol Sci 2008;106: 394-403.

[23]   Dong GZ, Lee JH, Ki SH, Yang JH, Cho IJ, Kang SH, Zhao RJ, Kim SC, Kim YW. AMPK activation by isorhamnetin protects hepatocytes against oxidative stress and mitochondrial dysfunction. Eur J Pharmacol 2014;740: 634-40.

[24]   Kong SS, Liu JJ, Yu XJ, Lu Y, Zang WJ. Protection against ischemia-induced oxidative stress conferred by vagal stimulation in the rat heart: involvement of the AMPK-PKC pathway. Int J Mol Sci 2012;13: 14311-25.

[25]   Ceolotto G, Gallo A, Papparella I, Franco L, Murphy E, Iori E, Pagnin E, Fadini GP, Albiero M, Semplicini A, Avogaro A. Rosiglitazone reduces glucose-induced oxidative stress mediated by NAD(P)H oxidase via AMPK-dependent mechanism. Arterioscler Thromb Vasc Biol 2007;27: 2627-33.

[26]   Cheng PW, Ho WY, Su YT, Lu PJ, Chen BZ, Cheng WH, Lu WH, Sun GC, Yeh TC, Hsiao M, Tseng CJ. Resveratrol decreases fructose-induced oxidative stress, mediated by NADPH oxidase via an AMPK-dependent mechanism. Br J Pharmacol 2014;171: 2739-50.

[27]   Bellido T. Osteocyte-driven bone remodeling. Calcif Tissue Int 2014;94: 25-34.

[28]   Tomkinson A, Gevers EF, Wit JM, Reeve J, Noble BS. The role of estrogen in the control of rat osteocyte apoptosis. J Bone Miner Res 1998;13: 1243-50.

[29]   Noble BS, Peet N, Stevens HY, Brabbs A, Mosley JR, Reilly GC, Reeve J, Skerry TM, Lanyon LE. Mechanical loading: biphasic osteocyte survival and targeting of osteoclasts for bone destruction in rat cortical bone. Am J Physiol Cell Physiol 2003;284: C934-43.

[30]   O'Brien CA, Jia D, Plotkin LI, Bellido T, Powers CC, Stewart SA, Manolagas SC, Weinstein RS. Glucocorticoids act directly on osteoblasts and osteocytes to induce their apoptosis and reduce bone formation and strength. Endocrinology 2004;145: 1835-41.

[31]   Jilka RL, Noble B, Weinstein RS. Osteocyte apoptosis. Bone 2013;54: 264-71.

[32]   Komori T. Mouse models for the evaluation of osteocyte functions. J Bone Metab 2014;21: 55-60.

[33]   Tang XQ, Shen XT, Huang YE, Ren YK, Chen RQ, Hu B, He JQ, Yin WL, Xu JH, Jiang ZS. Hydrogen sulfide antagonizes homocysteine-induced neurotoxicity in PC12 cells. Neurosci Res 2010;68: 241-9.

[34]   Sipkens JA, Hahn N, van den Brand CS, Meischl C, Cillessen SA, Smith DE, Juffermans LJ, Musters RJ, Roos D, Jakobs C, Blom HJ, Smulders YM, Krijnen PA, Stehouwer CD, Rauwerda JA, van Hinsbergh VW, Niessen HW. Homocysteine-induced apoptosis in endothelial cells coincides with nuclear NOX2 and peri-nuclear NOX4 activity. Cell Biochem Biophys 2013;67: 341-52.

[35]   Xu ZS, Wang XY, Xiao DM, Hu LF, Lu M, Wu ZY, Bian JS. Hydrogen sulfide protects MC3T3-E1 osteoblastic cells against H2O2-induced oxidative damage-implications for the treatment of osteoporosis. Free Radic Biol Med 2011;50: 1314-23.

[36]   Lee YS, Choi EM. Apocynin stimulates osteoblast differentiation and inhibits bone-resorbing mediators in MC3T3-E1 cells. Cell Immunol 2011;270: 224-9.

[37]   Barbieri SS, Cavalca V, Eligini S, Brambilla M, Caiani A, Tremoli E, Colli S. Apocynin prevents cyclooxygenase 2 expression in human monocytes through NADPH oxidase and glutathione redox-dependent mechanisms. Free Radic Biol Med 2004;37: 156-65.

[38]   Jia F, Wu C, Chen Z, Lu G. AMP-activated protein kinase inhibits homocysteine-induced dysfunction and apoptosis in endothelial progenitor cells. Cardiovasc Drugs Ther 2011;25: 21-9.

[39]   Rossi A, Lord JM. Adiponectin inhibits neutrophil apoptosis via activation of AMP kinase, PKB and ERK 1/2 MAP kinase. Apoptosis 2013;18: 1469-80.

[40]   Jia F, Wu C, Chen Z, Lu G. Atorvastatin inhibits homocysteine-induced endoplasmic reticulum stress through activation of AMP-activated protein kinase. Cardiovasc Ther 2012;30: 317-25.

[41]   Vestergaard P. Discrepancies in bone mineral density and fracture risk in patients with type 1 and type 2 diabetes--a meta-analysis. Osteoporos Int 2007;18: 427-44.

[42]   Yamamoto M, Yamaguchi T, Yamauchi M, Kaji H, Sugimoto T. Diabetic patients have an increased risk of vertebral fractures independent of BMD or diabetic complications. J Bone Miner

Res 2009;24: 702-9.

[43]   Li J, Zhang H, Yan L, Xie M, Chen J. Fracture is additionally attributed to hyperhomocysteinemia in men and premenopausal women with type 2 diabetes. J Diabetes Investig 2014;5: 236-41.

[44]   Vestergaard P, Rejnmark L, Mosekilde L. Relative fracture risk in patients with diabetes mellitus, and the impact of insulin and oral antidiabetic medication on relative fracture risk. Diabetologia 2005;48: 1292-9.

[45]   Melton LJ, 3rd, Leibson CL, Achenbach SJ, Therneau TM, Khosla S. Fracture risk in type 2 diabetes: update of a population-based study. J Bone Miner Res 2008;23: 1334-42.

[46]   Jang WG, Kim EJ, Lee KN, Son HJ, Koh JT. AMP-activated protein kinase (AMPK) positively regulates osteoblast differentiation via induction of Dlx5-dependent Runx2 expression in MC3T3E1 cells. Biochem Biophys Res Commun 2011;404: 1004-9.

[47]   Wang C, Li H, Chen SG, He JW, Sheng CJ, Cheng XY, Qu S, Wang KS, Lu ML, Yu YC. The skeletal effects of thiazolidinedione and metformin on insulin-resistant mice. J Bone Miner Metab 2012;30: 630-7.

[48]   Mai QG, Zhang ZM, Xu S, Lu M, Zhou RP, Zhao L, Jia CH, Wen ZH, Jin DD, Bai XC. Metformin stimulates osteoprotegerin and reduces RANKL expression in osteoblasts and ovariectomized rats. J Cell Biochem 2011;112: 2902-9.

Figure legends

Fig. 1

Effects of homocysteine on apoptosis of MLO-Y4 cells

DNA fragment detection ELISA analysis showed that homocysteine (Hcy) treatment significantly increased the apoptosis of MLO-Y4 cells in a dose-dependent manner (A). The result was representative of three different experiments. TUNEL staining showed that 5.0 mM Hcy increased the apoptosis of the cells. A representative picture is shown (B). Quantification of cell count of TUNEL-positive cells showed that difference was significant between control and Hcy treated cells (C). The result was representative of four different experiments. Results are expressed as the mean ± standard error of mean (SEM). *p < 0.05, **p < 0.01, and ***p < 0.001.

Fig. 2

Effects of an anti-oxidant, *N*-acetylcysteine, and NADPH oxidase inhibitors, apocynin and diphenyleneiodonium chloride, on homocysteine-induced apoptosis of MLO-Y4 cells

Apoptosis was evaluated by DNA fragment detection ELISA analysis. Treatment with 5 mM homocysteine (Hcy) significantly increased the apoptosis of MLO-Y4 cells. Co-incubation with 5 mM *N*-acetylcysteine (NAC) suppressed the Hcy-induced apoptosis (A). The result

was representative of three different experiments. Co-incubation with 0.1 mM apocynin (B) and 1.0 nM diphenyleneiodonium chloride (DPI) (C) partially but significantly decreased apoptosis induced by 5 mM homocysteine (Hcy). The result was representative of three different experiments. Results are expressed as the mean ± standard error of mean (SEM). *p < 0.05, **p < 0.01 and ***p < 0.001.

Fig. 3

Effects of AMPK activation on homocysteine-induced apoptosis of MLO-Y4 cells

Total RNA from the cells was subjected to RT-PCR, and the PCR products were visualized in a 1.8% agarose gel stained with ethidium bromide. We observed the expression of the mRNAs of all AMPK subunits α1, α2, β1, β2, γ1, γ2, and γ3 (A). DNA fragment ELISA assay showed that treatments with 5 mM homocysteine (Hcy) increased the apoptosis of MLO-Y4 cells, and co-incubation with AICAR (0.05 and 0.1 mM) significantly inhibited the Hcy-induced apoptosis (B). The result was the representative of four different experiments. TUNEL staining confirmed that 0.01 mM AICAR recovered the Hcy-induced apoptosis of the cells. A representative picture was shown (C). Quantification of cell count of TUNEL-positive cells showed that the differences were significant (D). The result was the representative of three different experiments. Effects of Metformin on the Hcy-induced apoptosis were examined by DNA fragment ELISA assay. Treatments with Met (10 and 100
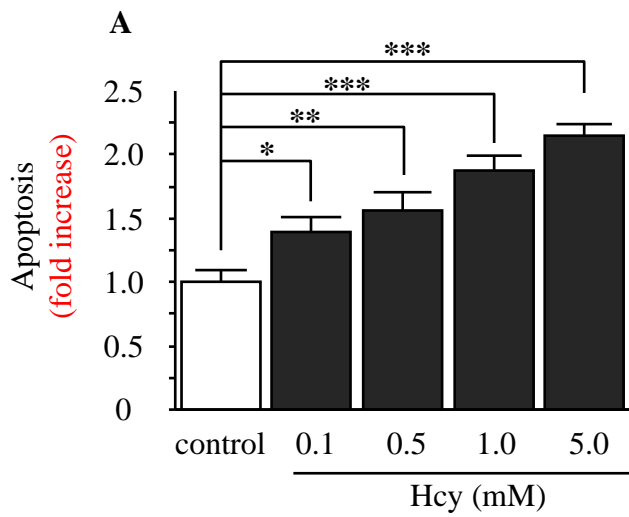
μM) significantly decreased the Hcy-induced apoptosis (E). Administration of 0.1 mM Ara-A inhibited the anti-apoptotic effects of metformin against Hcy (E). The result was the representative of three different experiments. Results are expressed as the mean ± SEM. **p<0.01, ***p<0.001.
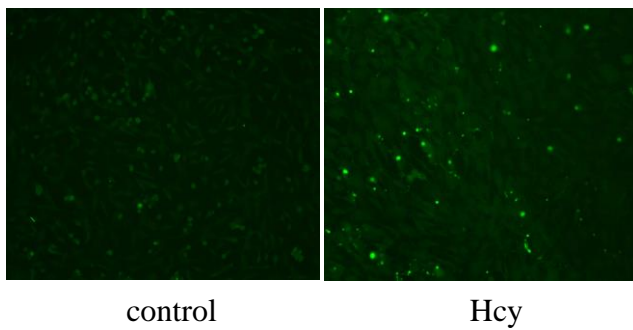
Fig. 4

Effects of Hcy and AICAR on expressions of Nox and SOD

Real-time PCR showed that 5 mM Hcy significantly increased Nox1 (A) and Nox2 (B) mRNA expressions. Co-incubation with 0.1 mM 5-aminoimidazole-4-carboxamide-1-β-D-ribofuranoside (AICAR) significantly decreased the Hcy-induced upregulation of NADPH oxidase 1 (Nox1) (A) and Nox2 (B). The expression of Nox4 (C) and superoxide dismutase 1 (SOD1) (D) mRNA was not affected by Hcy treatments. Results are expressed as the mean ± standard error of mean (SEM) (n > 6). **p < 0.01. Western blot analysis showed that treatments with 5 mM Hcy did not affect the protein expressions of SOD1 and SOD2 (E). The result was representative of three different experiments. Results are expressed as the mean ± SEM. *p < 0.05, **p<0.01, ***p<0.001.
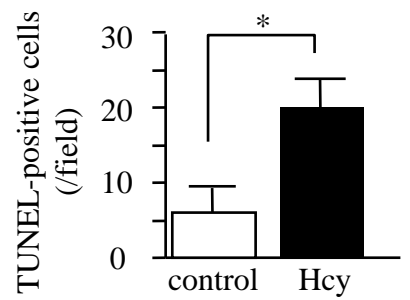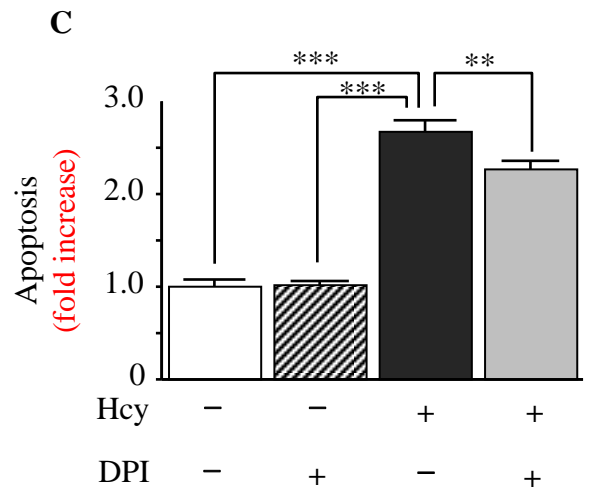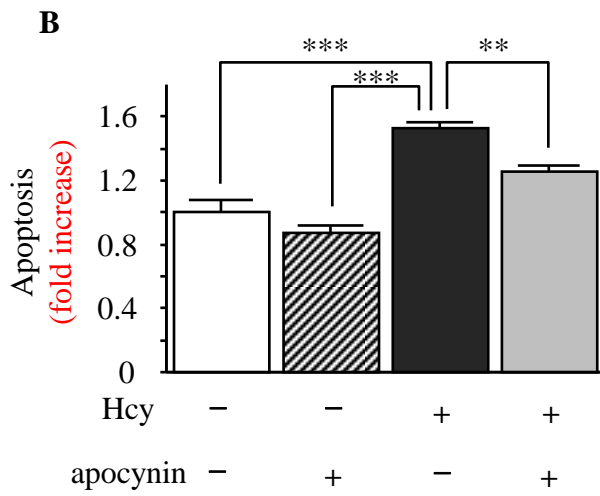
Fig.1

A

Apoptosis (fold increase)

Hcy (mM)

B

control   Hcy

C

TUNEL-positive cells (/field)

control   Hcy

Fig.2
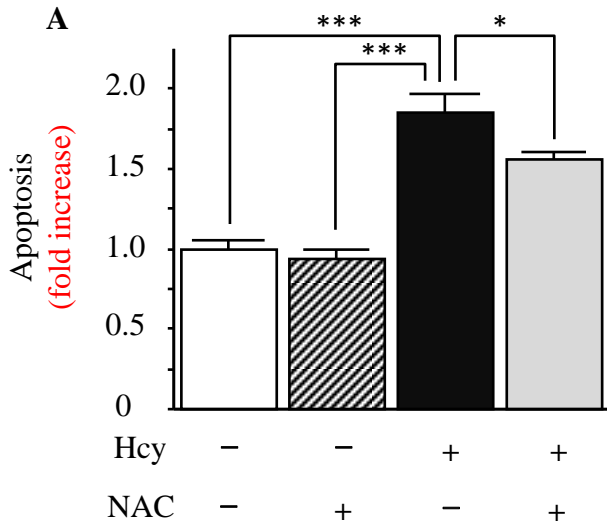
Fig.3
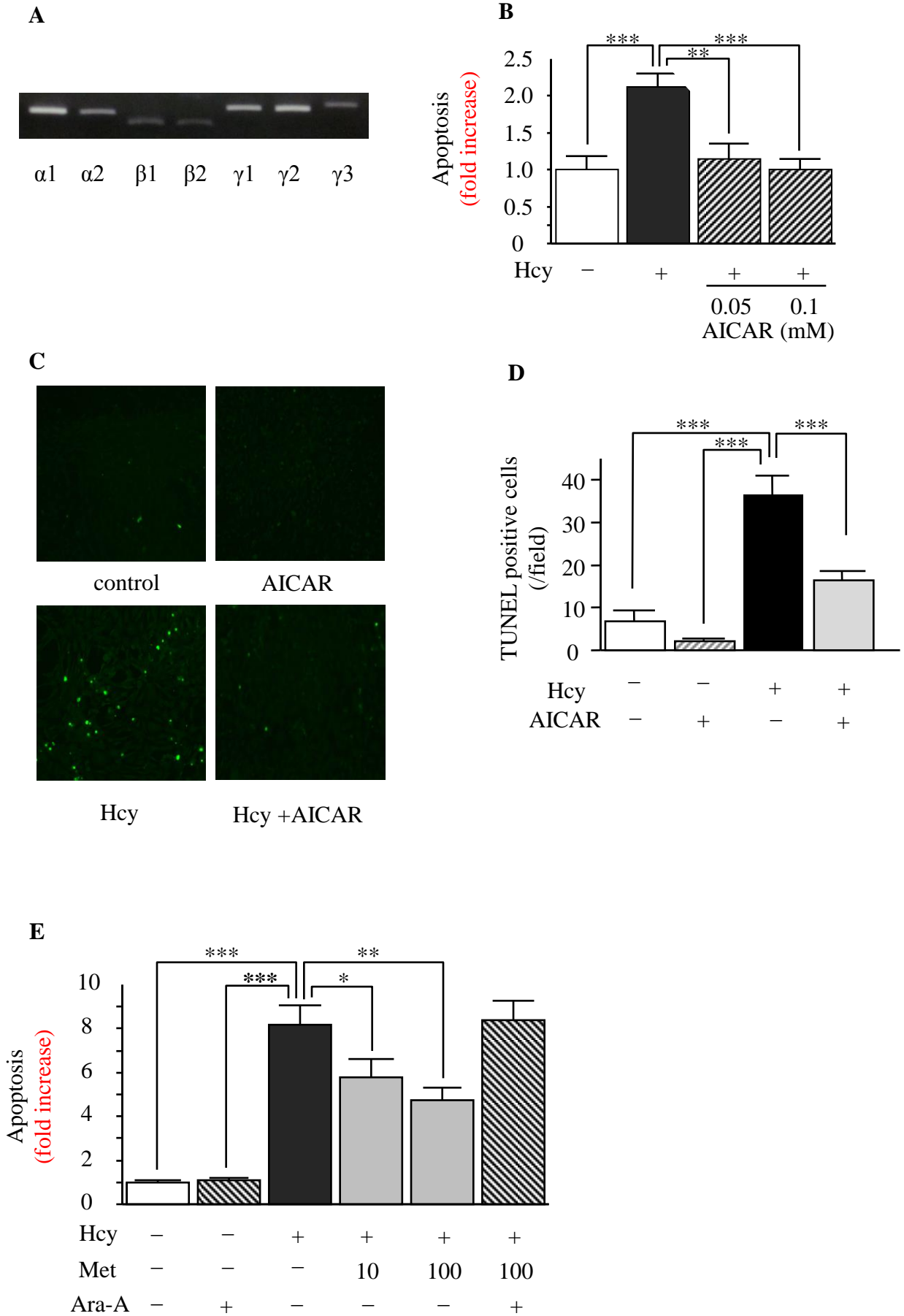
Fig.4
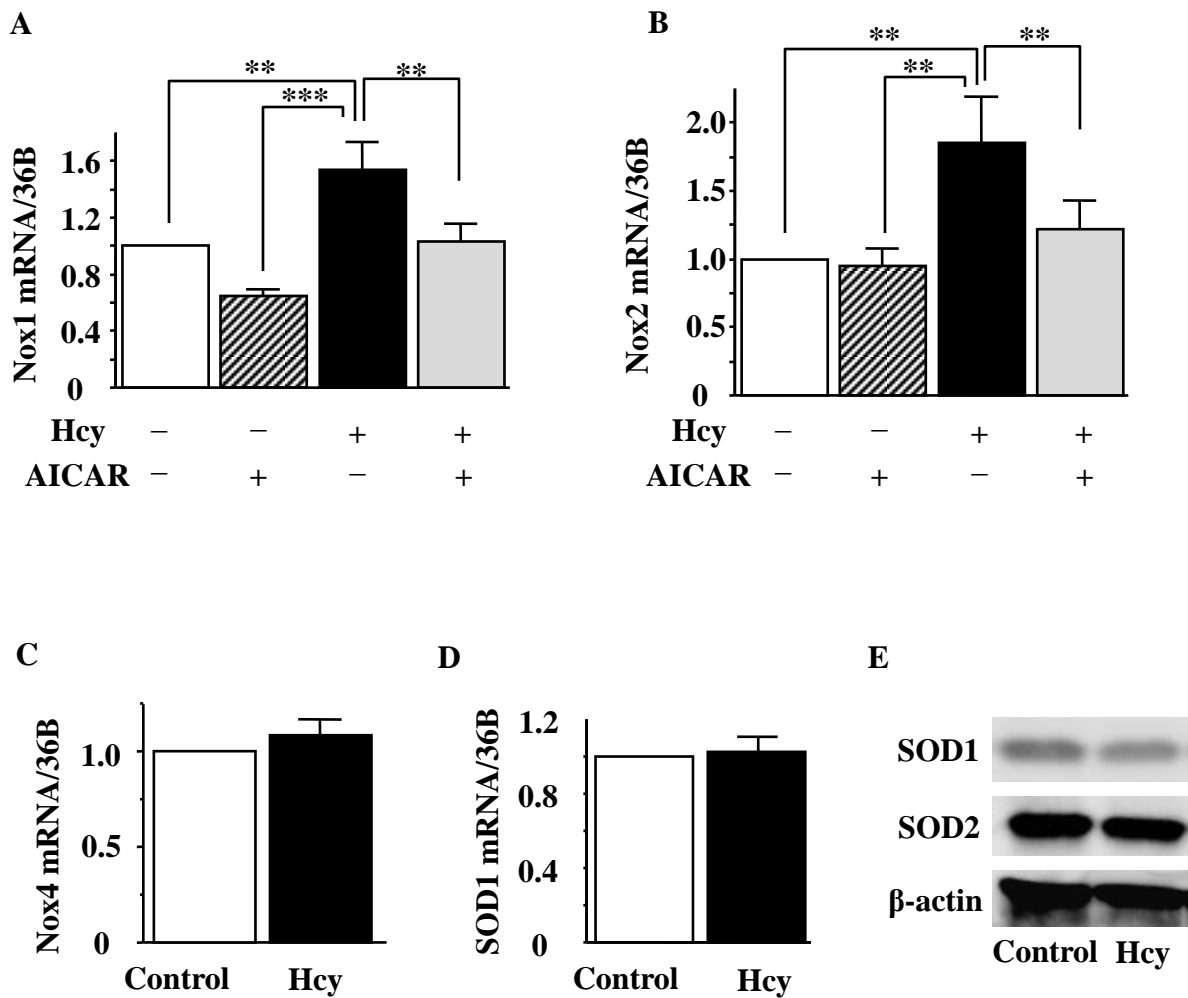
Table.1

Gene name	primers
AMPKα1	CTCTATGCTTTGCTGTGTGG
	GGTCCTGGTGGTTTCTGTTG
AMPKα2	ACAGCGCCATGCATATTCCT
	TCCGACTGTCTACCAGGTAA
AMPKβ1	TCAAGGATGGAGTGATGGTG
	GACTATGTGGGGGTGAGATG
AMPKβ2	AAACTCACTGGGCGAGGAAC
	CCACACAGCCAATACACAGG
AMPKγ1	GCTACAGATTGGCACCTACG
	TCAGGGCTTCTTCTCTCCAC
AMPKγ2	GCCTTCTTTGCTTTGGTAGC
	GCTCATCCAGGTTCTGCTTC
AMPKγ3	TCACCATCACGGACTTCATC
	CATCAAAGCGGGAGTAGAGG

Table.2

Gene name	primers
36B4	AAGCGCGTCCTGGCATTGTCT
	CCGCAGGGGCAGCAGTGGT
Nox1	ATGCCCCTGCTGCTCGAATA
	AAATTGCCCCTCCATTTCCT
Nox2	ACCGCCATCCACACAATTG
	CCGATGTCAGAGAGAGCTATTGAA
Nox4	CTGCATCTGTCCTGAACCTCAA
	TCTCCTGCTAGGGACCTTCTGT
SOD1	GGGTTCCACGTCCATCAGT
	CACACGATCTTCAATGGACAC